

Introduction

- In astrophysical and other applications, plasma is often in a **collisionless state**, where resistive/viscous effects are not dominating on the time/spatial scales of interest
- XMHD is thought to be important for the formation of **relativistic jets from active galactic nuclei, micro-quasars, and gamma-ray bursts** [1]
- Extended MHD (XMHD)** is formally 1-fluid model endowed with 2-fluid effects: **electron inertia** and **Hall drift** described by **IMHD** and **HMHD** limits respectively.
- These mutually exclusive effects were **unified in a covariant Hamiltonian model** [2].
- Eulerian action principle (AP) for relativistic XMHD is formulated so that constrained variations are generated by a degenerate Poisson bracket.
- For the first time, the Hamiltonian **formulation of relativistic HMHD** with **electron thermal inertia** is introduced [2]
- Relativistic HMHD (RHMHD)** allows the **violation of the frozen-in magnetic flux condition** via an **electron thermal inertia** effect [2]
- Energy and helicity cascades are studied in **non-relativistic 3D XMHD turbulence**
- Study addresses recent interest in **sub-electron scales** that have become observable.

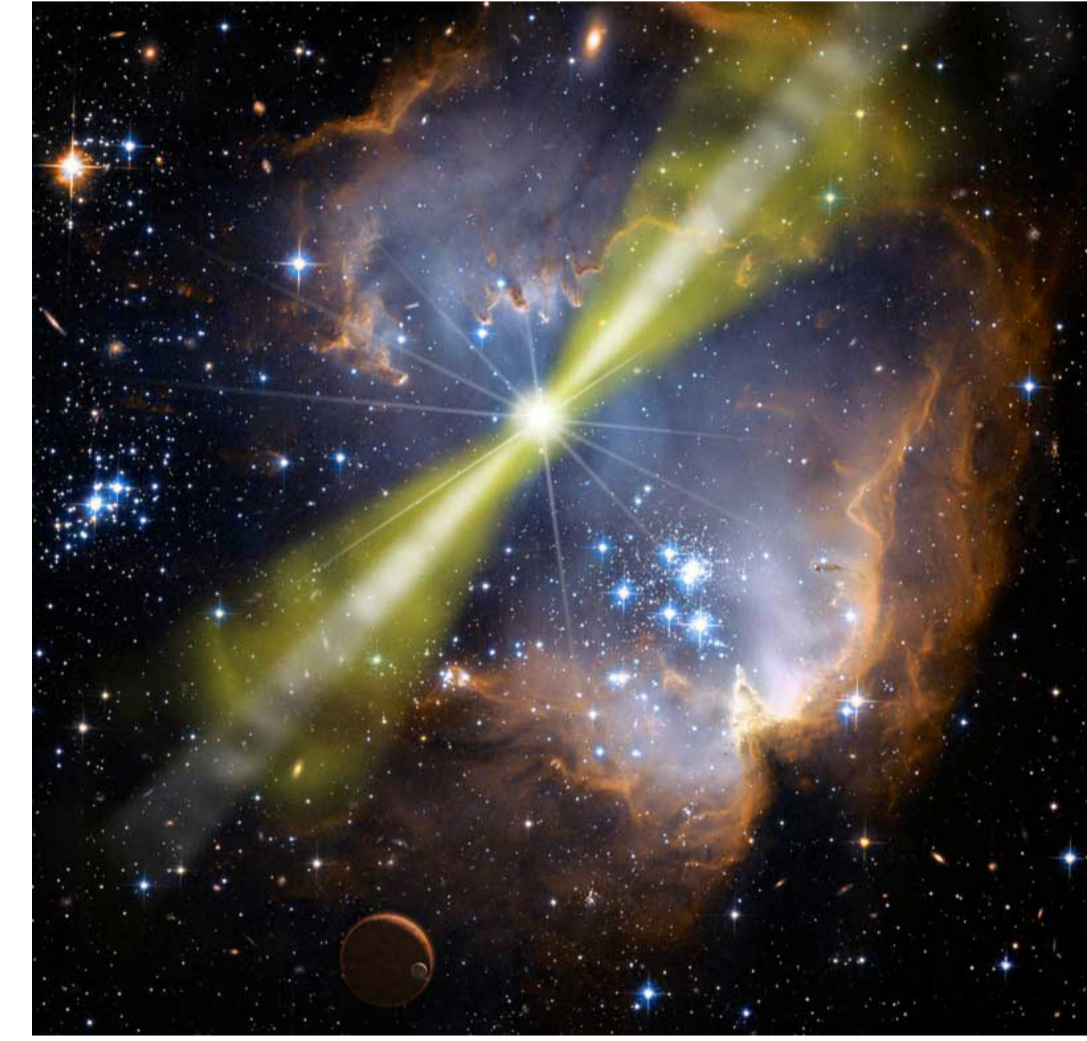


Figure: Artist's illustration of one model of the bright gamma-ray burst GRB 080319B

Advantages of Hamiltonian methods include:

- Systematic means for constructing equilibria, e.g. Beltrami flows.
- Clear derivation of reduced models avoiding introduction of spurious dissipation.
- Extraction of invariants such as helicity that plays a major role in this study.
- Understanding of how collisionless reconnection operates
- Natural means of arriving at weak turbulence theories.
- Construction of numerical integrators that automatically conserve invariants [4].

Constrained Least Action Principle

Introducing the action $S = \int \left[\frac{m^{*\nu} m_\nu}{2nh} + \sum_{\pm} \frac{1}{2} (p_{\pm} - \rho_{\pm}) - \frac{1}{4} \mathcal{F}^{*\mu\nu} \mathcal{F}_{\mu\nu} \right] d^4x$, (1)

where $A^{*\nu} := A^\nu + \frac{\Delta h}{e} u^\nu + \frac{h^\dagger}{ne^2} J^\nu$ and gen. momentum $m^{*\nu} := nh u^\nu + (\Delta h/e) J^\nu$ with enthalpies defined as $h := h_+ + h_-$, $\Delta h := (m_-/m)h_+ - (m_+/m)h_-$, and $h^\dagger := (m_-^2/m^2)h_+ + (m_+^2/m^2)h_-$. Starting from canonical Clebsch potentials

$$m^{*\nu} := n \partial^\nu \phi + \sum_{\pm} (\sigma_{\pm} \partial^\nu \eta_{\pm} + \lambda_{\pm} \partial^\nu \varphi_{\pm}), \quad A^{*\nu} := \sum_{\pm} \left[\pm \frac{m_{\pm}}{men} (\sigma_{\pm} \partial^\nu \eta_{\pm} + \lambda_{\pm} \partial^\nu \varphi_{\pm}) \right]$$

with **momenta** and **coordinates** entering the Poisson bracket. The least AP ($\delta S = 0$) is equivalent to a bracket AP, i.e., $\{F[z], S\} = 0$ where $F[z]$ is an arbitrary functional of Clebsch potentials. We affect coordinate change to $\bar{z} = (n, \sigma_{\pm}, m^{*\nu}, A^{*\nu})$ leading to

The corresponding covariant noncanonical bracket for relativistic XMHD

$$\{F, G\} = - \int \left\{ n \frac{\delta G}{\delta m^{*\nu}} \partial^\mu \frac{\delta F}{\delta n} + \sum_{\pm} \left[\sigma_{\pm} \frac{\delta G}{\delta m^{*\nu}} \partial^\mu \frac{\delta F}{\delta \sigma_{\pm}} \pm \frac{m_{\mp} \delta F}{me \delta \sigma_{\pm} \delta A^{*\nu}} \partial^\mu \sigma_{\pm} \right] + m^{*\nu} \frac{\delta G}{\delta m^{*\mu}} \partial^\mu \frac{\delta F}{\delta m^{*\nu}} + \mathcal{F}^{*\mu\nu} \frac{\delta F}{\delta A^{*\mu}} \frac{\delta G}{\delta A^{*\nu}} - \frac{1}{2ne} \frac{\delta F}{\delta A^{*\mu}} \frac{\delta G}{\delta A^{*\nu}} \mathcal{F}^{\dagger\mu\nu} - F \leftrightarrow G \right\} d^4x$$
 (2)

here $A^{\dagger\nu} := \frac{m_+ - m_-}{m} A^\nu - \frac{h^\dagger}{e} u^\nu - \frac{\Delta h^\dagger}{ne^2} J^\nu$, $\Delta h^\dagger := (m_-^3/m^3)h_+ - (m_+^3/m^3)h_-$ (3)

Limit to relativistic Hall MHD

Defining electron to ion mass ratio $\mu := m_e/m_i \rightarrow 0$. Applying following normalization:

$$\partial^\nu \rightarrow L^{-1} \partial^\nu, \quad n \rightarrow n_0 n, \quad T_{i,e} \rightarrow mc^2 T_{i,e}, \quad \mathcal{F}^{\mu\nu} \rightarrow \sqrt{n_0 mc^2} \mathcal{F}^{\mu\nu}, \quad c/(\omega_j L) = d_j$$

We substitute this into (2) and get **HMHD** bracket that generates equations:

$$\partial_\nu \left[nh u^\mu u^\nu - d_i h_e (u^\mu J^\nu + J^\mu u^\nu) + d_i^2 \frac{h_e}{n} J^\mu J^\nu \right] = \partial^\mu p + J^\nu \mathcal{F}^{\mu\nu}, \quad (4)$$

$$\left(u_\nu - d_i \frac{J_\nu}{n} \right) \mathcal{F}^{*\mu\nu} = -d_i T_e \partial^\mu \left(\frac{\sigma_e}{n} \right), \quad \partial_\nu (\sigma_i u^\nu) = 0 = \partial_\nu \left[\sigma_e \left(u^\nu - d_i \frac{J^\nu}{n} \right) \right] \quad (5)$$

The terms including h_e must not be ignored when $h_e \gg m_e c^2$ [2].

Relativistic Collisionless Reconnection

- In **IMHD**, **electron inertia** leads to the violation of the frozen-in magnetic flux.
- This effect was suggested as a **mechanism for collisionless magnetic reconnection** [5]
- However, nonrelativistic **HMHD** does satisfy the frozen-in magnetic flux condition
- In **RHMHD** with $\mu \rightarrow 0$ limit electron temperature may still be large enough to allow the violation of the frozen in condition and thus reconnection.
- In [6] the relativistic e-p plasma with the assumption $\Delta h = 0$ was considered.
- In **HMHD**, however, [2] $\Delta h = 0$ assumption removes the aforementioned mechanism.
- The **reconnection scale** is expected to be $\delta \sim \sqrt{h_e} d_i$, consistent with the e-p [6]

Models	frozen-in field
(R)MHD	B
HMHD	B
IMHD	$B + \nabla \times (d_e^2 J/n)$
RHMHD	$B + \nabla \times (-d_i h_e \gamma v + d_i^2 h_e J/n)$

Table: Induction equation for nonrelativistic and relativistic (R) models.

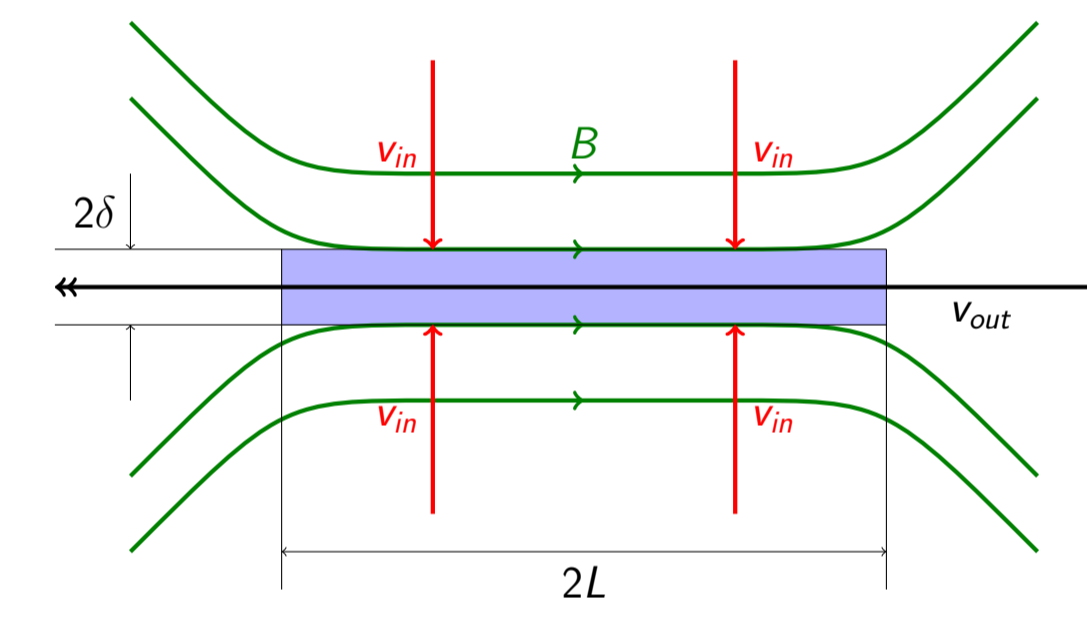


Figure: Geometry for Sweet-Parker reconnection model. Reconnection occurs in the blue layer and depends on the scale length δ .

Nonrelativistic XMHD – 3+1 decomposition

Upon rearranging the action (1) and applying relevant approximations for $v \ll c$

$$S = \int \frac{m_0 m^0}{2nmc^2} d^4x - \int dx^0 \int \underbrace{\left[-\frac{m_i m^i}{2nmc^2} + n \left(\frac{1}{2} mc^2 + \mathcal{E}_+ + \mathcal{E}_- \right) - \frac{A^{*i} J_i}{2} \right]}_{\text{Hamiltonian, } \mathcal{H}} d^3x \quad (6)$$

Performing **3+1 decomposition** $F = \int \delta(x^0 - x^{0'}) \mathcal{F}[n, \sigma_{\pm}, m^i, A^{*i}] dx^0 \Rightarrow$

$$\{F, S\} = \frac{1}{c} \int \left(\frac{\partial \mathcal{F}}{\partial t} - \underbrace{\left\{ \mathcal{F}, \mathcal{H} \right\}}_{\text{3D bracket}} \right) \delta(x^0 - x^{0'}) dx^0 + \int A^{*0} \underbrace{\partial^i \left(\frac{\delta \mathcal{F}}{\delta A^{*i}} \right)}_{\text{Evaluates to zero}} \delta(x^0 - x^{0'}) d^4x$$

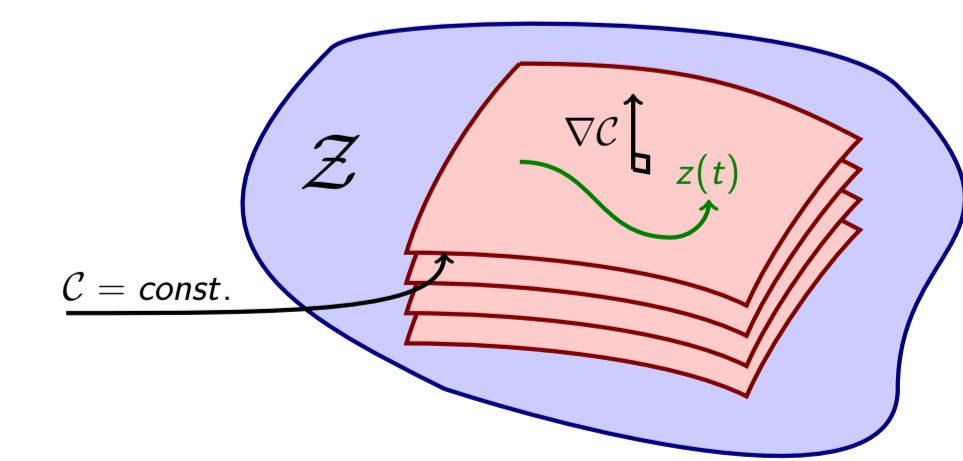


Figure: Foliation of phase space \mathcal{Z} by Casimirs C in finite dimensions. Observe how dynamical system evolves ($z = z(t)$) on individual Casimir leaves. But field theories like XMHD are uncountably infinite dimensional!

Seeking **Casimirs**: $\forall \mathcal{F} : 0 = \{ \mathcal{F}, C \} \Rightarrow$

$$C^{(\lambda)} = \int d^3x (A^{*i} + \lambda v^i) \cdot (B^{*i} + \lambda \nabla \times v^i),$$

where $\lambda_{\pm} := m_{\pm} c/e$. In addition when barotropic condition is violated we obtain the family (with the condition $f_{,+} = 0$)

$$C^{(\sigma)} = \int d^3x \varrho f \left(\frac{\sigma_+}{\varrho}, \frac{\sigma_-}{\varrho} \right), \quad (7)$$

3D Turbulence in nonrelativistic extended MHD

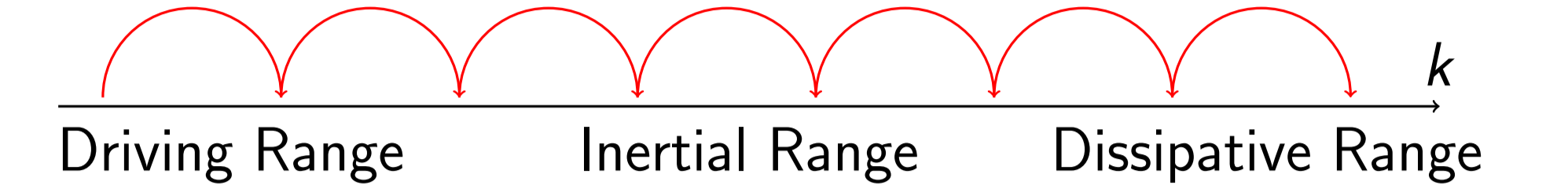


Figure: Schematics of a standard Richardson-Kolmogorov direct cascade. Energy is injected in low k , for e.g. via large scale stirring, cascades (flows) through the inertial range and dissipates at small scales (large k).

Symmetric two-point correlations (taken at x' and x) of generalized helicities

$$0 = \frac{\partial}{\partial t} \left[\underbrace{\langle \mathcal{A}'_{\pm} \cdot \mathcal{B}_{\pm} + \mathcal{A}_{\pm} \cdot \mathcal{B}'_{\pm} \rangle}_{\text{in a stationary regime, } \mathcal{A}'_{\pm} := \mathcal{A}_{\pm}(x') = A' + \lambda_{\pm} v'} \right] = - \underbrace{\langle \delta(\mathbf{V}_{\pm} \times \mathbf{B}_{\pm}) \cdot \delta \mathbf{B}_{\pm} \rangle}_{\text{helicity flux transfer rate}} + \underbrace{D}_{\text{damping}} \quad (8)$$

- More symmetry than in **HMHD**, where C_- has inverse and C_+ has both cascades [7].
- To determine direction of cascading we investigate **absolute equilibrium states** [3].
- Turbulence would relax into these states if not for the continual input of energy.
- To establish a bridge between MHD [8] and XMHD results we introduce Casimirs:

$$\text{magnetic- } H_M := \frac{1}{2} \frac{\kappa_+ C_- - \kappa_- C_+}{\kappa_+ - \kappa_-} = \frac{1}{2} \int d^3x (A^{*i} \cdot B^{*i} + d_e^2 \mathbf{V} \cdot \nabla \times \mathbf{V}), \quad (9)$$

$$\text{cross-helicity } H_C := \frac{1}{2} \frac{C_+ - C_-}{\kappa_+ - \kappa_-} = \int d^3x (\mathbf{V} \cdot B^{*i} + \frac{d_i}{2} \mathbf{V} \cdot \nabla \times \mathbf{V}), \quad (10)$$

$$\text{Phase space probability density } \mathcal{P} = Z^{-1} \exp[-\alpha H - \beta H_M - \gamma H_C] \quad (11)$$

The resulting states are plotted, for **HMHD** set $d_e = 0$, **IMHD** - $d_i = 0$;

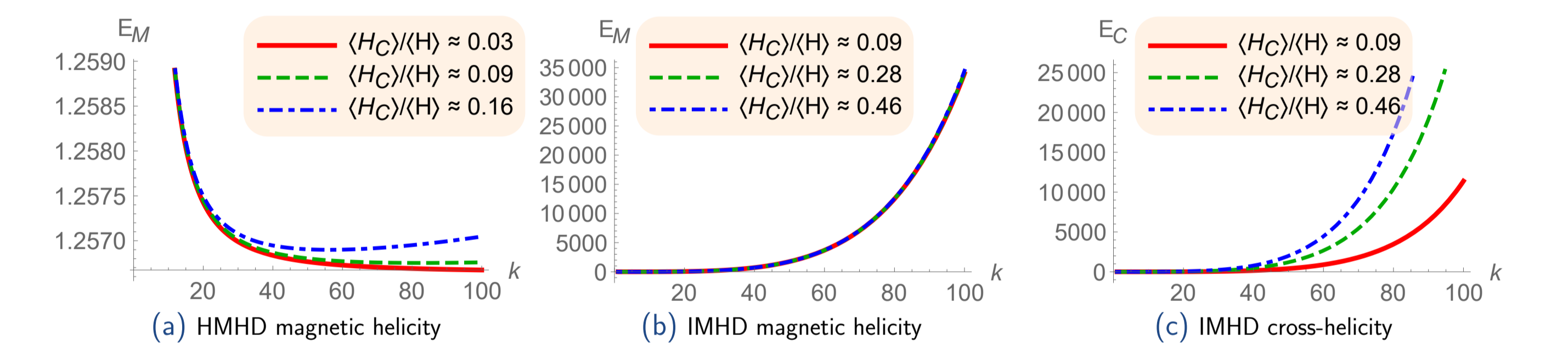


Figure: Absolute equilibria states of spectral quantities, e.g. $E_M := 4\pi k^2 \langle H_M \rangle_k$ and $\langle H \rangle := \int E dk$. Parameters $\alpha = 10$, $\beta = 5$ and γ is varied. (a) The **HMHD** regime, $d_i = 0.1$. (b) **IMHD** magnetic helicity. (c) **IMHD** cross-helicity with $d_e = 0.1$.

- Inverse cascade** is predicted only for magnetic helicity in **HMHD** range if $H_C \ll H$.
- IMHD** range is characterized by **direct cascades** for energy, and both helicities.
- IMHD** model differs from [9] where direct cascades were obtained for electron MHD.

Short Summary

We described APs for relativistic XMHD using **noncanonical covariant Poisson bracket**. In addition we formulated relativistic HMHD, obtained by taking a limit of the AP for XMHD. We observed that while nonrelativistic HMHD does not have a direct mechanism for collisionless reconnection, relativistic HMHD does allow the violation of the frozen-in magnetic flux condition via the electron thermal inertia effect. We estimated the resulting **reconnection scale**. Next we studied some general properties of non-relativistic XMHD turbulence. We expect that the (generalized) magnetic helicity undergoes inverse cascade up to a certain length scale (for a given choice of the free parameters), and then undergoes a **cascade reversal**. When electron inertia effects are taken to be dominant over the Hall term (IMHD regime operating on shorter sub-electron scales) we find that energy equipartition that was lost in HMHD is recovered.

References

- [1] S. Koide, The Astroph. J. 696 (2), (2009)
- [2] Y. Kawazura, G. Miloshevich, P.J. Morrison Phys. Plasmas 24, 022103 (2017)
- [3] G. Miloshevich, M. Lingam and P.J. Morrison New J. Phys. 19 (1), 015007, (2017)
- [4] P.J. Morrison Phys. Plasmas, accepted (2017)
- [5] M. Ottaviani, F. Porcelli Phys. Rev. Lett. 71, 3802, (1993)
- [6] L. Comisso and F. A. Asenjo Phys. Rev. Lett. 113, 045001 (2014)
- [7] S. Benerjee and S. Galtier, Phys. Rev. E, 93, 033120 (2016)
- [8] U. Frisch, A. Pouquet, J. Liorat, and A. Mazure J. Fluid. Mech., 68, 769 (1975)
- [9] J.Z. Zhu arXiv:1703.01705 [physics.plasm-ph]